Title

Hyperpolarized NMR study of the impact of pyruvate dehydrogenase kinase inhibition on the pyruvate dehydrogenase and TCA flux in type 2 diabetic rat muscle

Journal

Pflügers Archiv - European Journal of Physiology, 473(11)

ISSN

0031-6768

Authors

Park, Jae Mo
Josan, Sonal
Hurd, Ralph E
et al.

Publication Date

2021-11-01

DOI

10.1007/s00424-021-02613-3

Peer reviewed

Pflügers Archiv - European Journal of Physiology
https://doi.org/10.1007/s00424-021-02613-3

MOLECULAR AND CELLULAR MECHANISMS OF DISEASE

Hyperpolarized NMR study of the impact of pyruvate dehydrogenase kinase inhibition on the pyruvate dehydrogenase and TCA flux in type 2 diabetic rat muscle

Jae Mo Park[1,2] · Sonal Josan[2,3] · Ralph E. Hurd[2,4] · James Graham[5] · Peter J. Havel[5] · David Bendahan[6] · Dirk Mayer[3,7] · Youngran Chung[8] · Daniel M. Spielman[2] · Thomas Jue[8]

Received: 25 May 2021 / Revised: 9 August 2021 / Accepted: 10 August 2021

Abstract

The role of pyruvate dehydrogenase in mediating lipid-induced insulin resistance stands as a central question in the pathogenesis of type 2 diabetes mellitus. Many researchers have invoked the Randle hypothesis to explain the reduced glucose disposal in skeletal muscle by envisioning an elevated acetyl CoA pool arising from increased oxidation of fatty acids. Over the years, in vivo NMR studies have challenged that monolithic view. The advent of the dissolution dynamic nuclear polarization NMR technique and a unique type 2 diabetic rat model provides an opportunity to clarify. Dynamic nuclear polarization enhances dramatically the NMR signal sensitivity and allows the measurement of metabolic kinetics in vivo. Diabetic muscle has much lower pyruvate dehydrogenase activity than control muscle, as evidenced in the conversion of [1-^{13}C] lactate and [2-^{13}C]pyruvate to HCO_3^- and acetyl carnitine. The pyruvate dehydrogenase kinase inhibitor, dichloroacetate, restores rapidly the diabetic pyruvate dehydrogenase activity to control level. However, diabetic muscle has a much larger dynamic change in pyruvate dehydrogenase flux than control. The dichloroacetate-induced surge in pyruvate dehydrogenase activity produces a differential amount of acetyl carnitine but does not affect the tricarboxylic acid flux. Further studies can now proceed with the dynamic nuclear polarization approach and a unique rat model to interrogate closely the biochemical mechanism interfacing oxidative metabolism with insulin resistance and metabolic inflexibility.

Keywords Type 2 diabetes · Skeletal muscle · Lactate · Dichloroacetate · Hyperpolarized NMR · Metabolism

Abbreviations

IRS	Insulin receptor substrate
IMCL	Intramuscular lipid
T2DM	Type 2 diabetes mellitus
DNP	Dynamic nuclear polarization
PDH	Pyruvate dehydrogenase
DCA	Dichloroacetate
PFK	Phosphofructokinase
G6P	Glucose 6 phosphate
PGC-1α	Peroxisome proliferator-activated receptor-γ coactivator 1α
PDK	Pyruvate dehydrogenase kinase
DKO	Double knock-out
ETC	Electron transport chain

✉ Thomas Jue
tjue@ucdavis.edu

[1] Advanced Imaging Research Center, University of Texas Southwestern Medical Center, 5323 Harry Hines Blvd., Dallas, TX 75390, USA

[2] Department of Radiology, Stanford University, 1201 Welch Rd., Stanford, CA 94305, USA

[3] Neuroscience Program, SRI International, 333 Ravenswood Ave., Menlo Park, CA 94025, USA

[4] Applied Science Laboratory, GE Healthcare, 333 Ravenswood Ave., Menlo Park, CA 94025, USA

[5] Department of Molecular Biosciences, University of California Davis, 3426 Meyer Hall, Davis, CA 95616, USA

[6] CNRS, Aix-Marseille University, CRMBM, 13385 Marseille, France

[7] Department of Diagnostic Radiology and Nuclear Medicine, University of Maryland, 22 S. Green St., Baltimore, MD 21201, USA

[8] Department of Biochemistry and Molecular Medicine, University of California-Davis, 4323 Tupper Hall, Davis, CA 95616, USA

Published online: 20 August 2021

tC	Total ^{13}C signal
ALCAR	Acetyl carnitine
AcAc	Acetoacetate
LDH	Lactate dehydrogenase
ALT	Alanine aminotransferase
TCA	Tricarboxylic acid
CrAT	Carnitine acetyl transferase

Introduction

Pyruvate dehydrogenase (PDH) stands at the crossroads directing the flux of non-oxidative and oxidative metabolism in skeletal muscle. Because of its unique position in metabolism, researchers have posited a significant role in regulating the dynamic metabolic response in muscle contraction and in selecting fuel source, especially in type 2 diabetes mellitus (T2DM) [61, 64, 69]. How PDH activity links lipid-carbohydrate metabolism to insulin resistance in skeletal muscle, however, remains incompletely understood. Does elevated fatty acid oxidation in T2DM increase the acetyl CoA level to impair PDH activity and to reduce glucose transport by inhibiting phosphofructokinase (PFK) as proposed by Randle 50 years ago [51]? ^{31}P NMR studies appear to militate against such a hypothesis, since they do not detect the expected increased glucose 6 phosphate (G6P) in T2DM muscle [53]. Neither lipid infusion nor hyperglycemia-hyperinsulinemia produces elevated G6P in T2DM muscle [9, 52]. Instead, T2DM muscle exhibits a much lower level of G6P than normal muscle, consistent with the decreased glycogen synthesis rate [59].

Despite the uncertainty in PDH mechanism interfacing the glucose-lipid cycle and the cautionary note from metabolic control theory, studies have nevertheless proposed stimulating PDH with a pyruvate dehydrogenase kinase (PDK) inhibitor as a therapeutic [16, 19, 63]. However, extant measurements cannot assess directly PDH kinetics in vivo. Indeed, with constitutively inhibited PDK, the double knock-out (DKO) pyruvate dehydrogenase kinase 2 (PDK2) and pyruvate dehydrogenase 4 (PDK4) mouse model continues to exhibit significant insulin resistance [50]. The observation raises the question about the specific role of PDH in insulin resistance, since bioactive lipid intermediates can directly impair insulin receptor substrate (IRS) to reduce glucose transport [21, 55].

To clarify the role of PDH requires measuring PDH activity in vivo, which has posed a daunting technical challenge. Even the most sophisticated NMR methodology can only determine a steady-state ratio of PDH flux (V_{PDH}) to the tricarboxylic acid (TCA) flux (V_{TCA}) based on ^{13}C fractional enrichment in the alanine and glutamate pools [58]. Indeed, the limitation in observing PDH flux in vivo confines scientific investigation to downstream metabolic effect or analysis of biopsied tissue. Because of the methodological limitation, experiments cannot assess critically the equilibrium between the acetyl CoA and acetyl carnitine (ALCAR), which buffers acetyl CoA availability [66].

Using dynamic nuclear polarization (DNP) NMR and a T2DM rat model, the present study has captured insight into the PDH flux in skeletal muscle during PDK inhibition. Previous DNP studies have already established that the hyperpolarized NMR approach can map the PDH activity in perfused heart from streptozotocin-treated animals [29]. It has the capacity to even measure PDH flux in human muscle [38]. Because DNP NMR has a much greater signal sensitivity than conventional NMR, it can track the rapid biodistribution/metabolism of ^{13}C precursors and follow the dynamic conversion of [2-^{13}C]pyruvate and [1-^{13}C]lactate into acetyl CoA as reflected in the bicarbonate (HCO_3^-) and into ALCAR [2, 39, 40].

In addition, a unique rat model T2DM model (UCD_T2DM) provides a convenient way to contrast PDH activities, because the UCD_T2DM model develops increasing adult-onset obesity and insulin resistance in the pre-diabetic state and progresses to overt diabetes with ß-cell dysfunction and fasting and non-fasting hyperglycemia [11]. Unlike other diabetes animal models, the UCD_T2DM model follows the T2DM pathogenesis observed in humans. The rat exhibits polygenic adult-onset leading to peripheral insulin resistance, inadequate β-cell compensation, and intact leptin signaling [10, 26].

Indeed, the results show that T2DM muscle has a lower resting PDH activity than CRL muscle. Introducing dichloroacetate (DCA) restores the T2DM PDH activity to match the CRL level, but the restored PDH flux shunts a significant fraction of the acetyl CoA into the ALCAR pool [63]. The increased PDH flux does not increase correspondingly the TCA flux as reflected in the ^{13}C labeling of glutamate. PDK inhibition certainly restores PDH activity in T2DM to normal level, but it does not enhance correspondingly the TCA flux. Other metabolic steps in the electron transport chain (ETC), oxidative phosphorylation, and carnitine acetyl transferase (CrAT) appear to intervene.

Materials and methods

^{13}C substrate and dynamic nuclear polarization

Samples of [1-^{13}C]lactate and [2-^{13}C]pyruvate were separately polarized using HyperSense DNP system (Oxford Instruments Molecular Biotools, Oxford, UK), which operates at 1.4 K of temperature and 25 mW of microwave power in a 3.35 T magnet. [1-^{13}C]Lactate sample was prepared by mixing 90 mg of 2.1-M sodium [1-^{13}C] lactate with 15-mM OX063 trityl radical with 10 µL of

a 1:50 dilution of Dotarem (Guerbet, France). When the solid-state polarization level reached a plateau (~ 3 h of polarization time), the lactate sample was dissolved in 5 g of 40-mM Tris buffer containing 100-mg/L disodium ethylenediaminetetraacetic acid (EDTA-Na_2), resulting in a final solution of 40-mM lactate. For [2-^{13}C]pyruvate sample, 25 µL of 14-M [2-^{13}C]pyruvate, mixed with the 15-mM OX063 trityl radical and 3 µL of diluted Dotarem. After the solid-state polarization is saturated (~ 1.5 h), the sample was dissolved into 4.5 g of 80-mM NaOH solution with 40-mM Tris buffer and 100-mg/L EDTA-Na_2 to yield an 80-mM solution of hyperpolarized pyruvate at a pH ~ 7.5 [1].

Animal preparation

Animal care and experimental procedures followed the guidelines of the National Institute of Health Office for Laboratory Animal Welfare and were approved by the local Institutional Animal Care and Use Committee. UCD_T2DM (505–640 g, $N = 6$) and age and weight-matched CRL Sprague–Dawley rats (520–656 g, $N = 7$) were prepared. Each rat was anesthetized (1–3% isoflurane in 1.5 L/min oxygen) and catheterized in tail vein, followed by positioning a custom-made transmit/receive ^{13}C radiofrequency (RF) surface coil (diameter $\varnothing = 28$ mm) on top of right rectus femoris, which was placed inside a ^{1}H transmit/receive birdcage coil ($\varnothing = 70$ mm). Vital signs such as respiration, oxygenation saturation, and temperature were monitored throughout the experiments. Adjusting the isoflurane level and the temperature of a warm water blanket maintained the respiration and body temperature at ~ 60 breaths/min and ~ 37 °C.

[1-^{13}C]Lactate (0.78 mmol/kg body weight) and [2-^{13}C]pyruvate (1.56 mmol/kg) injections were performed in separate groups of animals (three T2DM and four control rats for [1-^{13}C]lactate, three T2DM and three control rats for [2-^{13}C]pyruvate). Each rat was administered a solution with hyperpolarized ^{13}C-substrate at a rate of 0.25 mL/s with concurrent ^{13}C data acquisition. Moreover, each animal was scanned again following the same injection of hyperpolarized ^{13}C-substrate 1 h after a DCA infusion (200 mg/kg, dissolved in 30 g/mL of saline). DCA upregulated PDH activity by inhibiting PDK [63].

Hyperpolarized [1-^{13}C]lactate was used (1) to evaluate feasibility of differentiating PDH activity in normal and diabetic muscle metabolism and (2) to assess the effects of PDH activity change by adding DCA. Hyperpolarized [2-^{13}C]pyruvate was used to assess the fate of the increased pyruvate flux into mitochondrial metabolism [57].

MR protocol

After acquiring proton (^{1}H) anatomical references, B_0 field inhomogeneity over the targeted skeletal muscle region was reduced by minimizing the linewidth of the unsuppressed water signal of the muscle using the linear shim currents and a ^{1}H point-resolved spectroscopy sequence. Metabolic kinetics were measured from time-resolved ^{13}C NMR data, acquired using a dynamic free induction decay MR sequence (non-selective excitation, flip angle = 10°, temporal resolution = 3 s, spectral width/points = 10 kHz/4,096, acquisition time = 4 min) [40].

Data processing and analysis

The acquired ^{13}C data were apodized by a Gaussian filter (5 Hz) and zero-filled by a factor of four along the spectral dimension, followed by a fast Fourier transform and zeroth order spectral phase correction using MATLAB (Mathworks, Inc., Natick, MA, USA). Metabolite levels were assessed by integrating the respective peak in the absorption mode from time-averaged spectra (0–2 min). Metabolite ratios relative to the total ^{13}C signal (tC), which is the sum of all the ^{13}C-labeled signals, were used to compare metabolism in T2DM and CRL rats, and to assess the DCA effects.

Dynamic analysis of each metabolite was performed from the peak integrals of the time-resolved spectra to estimate metabolite production rate using two parameters: initial mean slope and half-maximum time. The production rate was estimated from the mean slope (r) of the four initial time points that appeared in the dynamic curves, which was then normalized to the initial mean slope of the injected substrate. The time where the half-maximum of each metabolite is achieved (τ) was also measured to assess the metabolite production rate [56].

The statistical significance of DCA effects on metabolic changes was evaluated using a paired Student's t-test for CRL and T2DM rats with respect to DCA (two-tailed analysis, $\alpha = 0.05$). The metabolic differences between CRL and T2DM and rats were statistically compared using an unpaired Student's t-test (two-tailed, $\alpha = 0.05$). All values were reported as mean ± standard error. Statistical significance was assigned when the analysis power equals or exceeds 0.8 and $P \leq 0.05$.

Results

Hyperpolarized [1-^{13}C]lactate

As shown in the representative time-averaged spectra (Fig. 1), the injection of [1-^{13}C]lactate produced pyruvate/tC (pyr/tC) and alanine/tC (ala/tC). In control

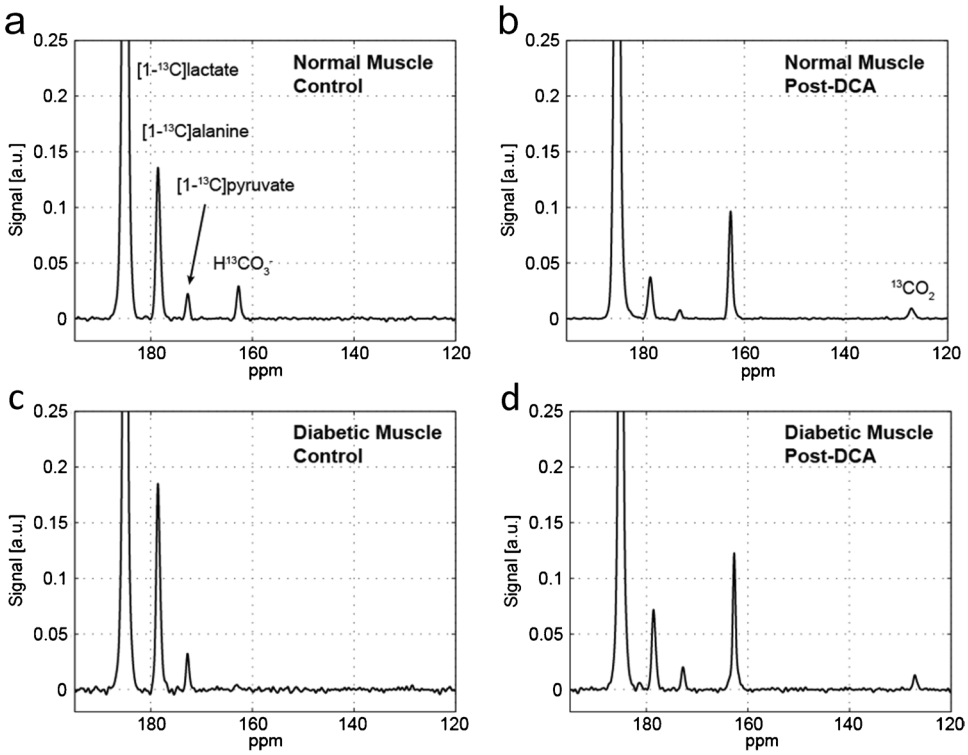

Fig. 1 Time averaged spectra from representative healthy and diabetic rat leg muscle after an injection of hyperpolarized 40-mM [1-^{13}C]lactate. (a) Normal muscle control, (b) normal muscle post-DCA, (c) diabetic muscle control, and (d) diabetic muscle post-DCA

muscle, the corresponding pyr/tC and ala/tC values showed 0.028 ± 0.002 and 0.129 ± 0.011, respectively. In T2DM muscle, the ala/tC values showed 0.026 ± 0.002 and 0.153 ± 0.010, respectively. T2DM did not alter the lactate conversion to pyruvate but appears to increase slightly the conversion to ala. T2DM muscle exhibited a significantly lower HCO_3^- signal ($P = 0.02$): CRL (0.012 ± 0.003); T2DM (0.002 ± 0.001). With the addition of DCA, HCO_3^- levels increased in both CRL and T2DM muscles: CRL (0.076 ± 0.005); T2DM (0.087 ± 0.011) [3]. Even though HCO_3^-/tC increased to approximately the same level in CRL and T2DM muscle, DCA induced a much larger dynamic change in T2DM as indicated by the ratio of HCO_3^-/tC with DCA over HCO_3^-/tC without DCA: CRL $0.076/0.012 = 6.3$; T2DM $0.087/0.002 = 43.5$. As DCA increased HCO_3^- conversion, it also decreased sharply pyruvate and alanine levels (Table 1).

As illustrated in Fig. 2, the dynamic parameters corroborated a similar trend. The relative metabolite production rate from lactate to HCO_3^- ($r_{lac \rightarrow bic}$) appeared higher ($P = 0.05$) in control (0.018 ± 0.004) than in T2DM muscle (0.007 ± 0.003). DCA increased $r_{lac \rightarrow bic}$ in both groups ($P < 0.002$). The production rate from lactate to alanine ($r_{lac \rightarrow ala}$) was also apparently higher in CRL than T2DM ($P = 0.08$). Both groups showed a drop in $r_{lac \rightarrow ala}$ after the addition of DCA. CRL showed a smaller relative change than T2DM (34% for CRL, 62% for T2DM). The metabolite production rates of pyruvate ($r_{lac \rightarrow pyr}$) were comparable between CRL and T2DM both pre- and post-DCA. Build-up times of in vivo hyperpolarized signal to half maximum were at similar levels between CRL and T2DM for pyruvate ($\tau_{lac \rightarrow pyr}$) and alanine ($\tau_{lac \rightarrow ala}$), while $\tau_{lac \rightarrow bic}$ was only measurable in CRL due to its low signal-to-noise ratio (SNR) in T2DM muscle. However, alanine ($P = 0.006$) and HCO_3^- ($P = 0.1$) built up faster in T2DM than in CRL in the presence of DCA (Table 1).

Hyperpolarized [2-^{13}C]pyruvate

When hyperpolarized [2-^{13}C]pyruvate was injected, neither CRL nor T2DM showed reliable mitochondrial metabolite peaks ([1-^{13}C]ALCAR, [1-^{13}C]acetoacetate (AcAc), and [5-^{13}C]glutamate signals) (Fig. 3). With DCA, these signals were consistently observed [57]. In T2DM muscle, DCA addition produced a much higher level of ALCAR (ALCAR/tC $= 0.079 \pm 0.009$, $P < 0.04$) and AcAc (AcAc/tC $= 0.037 \pm 0.004$, $P < 0.03$) than CRL. These values were 2 times higher than the values observed in CRL muscle (ALCAR/tC $= 0.044 \pm 0.004$, AcAc/tC $= 0.018 \pm 0.004$). However, glutamate/tC signals were comparable between T2DM (0.010 ± 0.003) and CRL (0.011 ± 0.001, $P > 0.9$). Without DCA, T2DM muscle converted more [2-^{13}C]pyruvate to [2-^{13}C]lactate (lac/tC $= 0.060 \pm 0.003$) than control muscle (0.040 ± 0.006). With DCA, T2DM and control muscle produced comparable amounts of [2-^{13}C]lactate (Table 2).

Table 1 Hyperpolarized [1-^{13}C] lactate metabolite distribution in control and T2DM rat leg muscle

	Baseline, No DCA		Post-DCA	
	Control	T2DM	Control	T2DM
Metabolite/total carbon				
HCO_3^-/tC	0.012 ± 0.003	0.002 ± 0.001	0.076 ± 0.005	0.087 ± 0.011
Lactate/tC	0.812 ± 0.013	0.821 ± 0.011	0.865 ± 0.009	0.909 ± 0.006
Pyruvate/tC	0.028 ± 0.002	0.026 ± 0.002	0.0088 ± 0.0003	0.015 ± 0.002
Alanine/tC	0.129 ± 0.011	0.153 ± 0.010	0.050 ± 0.004	0.075 ± 0.005
Metabolite ratio				
Pyruvate/alanine	0.224	0.173	0.178	0.199
Alanine/pyruvate	4.464	5.780	5.618	5.025
Lactate/pyruvate	29.000	31.577	98.295	60.600
HCO_3^-/pyruvate	0.429	0.077	8.636	5.800
Alanine/lactate	1.589	1.864	5.780	8.251
Relative metabolite production rate				
$r_{lac\rightarrow bic}$	0.018 ± 0.004	0.007 ± 0.003	0.132 ± 0.033	0.033 ± 0.003
$r_{lac\rightarrow pyr}$	0.055 ± 0.011	0.054 ± 0.009	0.021 ± 0.009	0.027 ± 0.009
$r_{lac\rightarrow ala}$	0.139 ± 0.026	0.082 ± 0.014	0.092 ± 0.027	0.031 ± 0.013
Time to half maximum [s]				
$\tau_{lac\rightarrow bic}$	17.4 ± 1.1	N.D	14.6 ± 0.4	16.2 ± 1.1
$\tau_{lac\rightarrow pyr}$	12.8 ± 0.7	12.3 ± 0.7	10.7 ± 0.3	12.0 ± 1.0
$\tau_{lac\rightarrow ala}$	18.0 ± 0.9	19.2 ± 0.6	14.1 ± 1.0	19.3 ± 0.9

Statistically significant paired *t*-test ($P \leq 0.05$) and power ≥ 0.8:

Control v Control -DCA: HCO_3^-, Lac, Pyr, Ala, $r_{lac\rightarrow bic}$, $\tau_{lac\rightarrow ala}$; T2DM v T2DM-DCA: HCO3$^-$, Lac, Pyr, Ala, $r_{lac\rightarrow bic}$

Statistically significant unpaired *t*-test ($P \leq 0.05$) and power ≥ 0.8:

Control v T2DM: HCO_3^-; Control-DCA v T2DM-DCA: Lac, Pyr, Ala, $r_{lac\rightarrow bic}$, $\tau_{lac\rightarrow ala}$

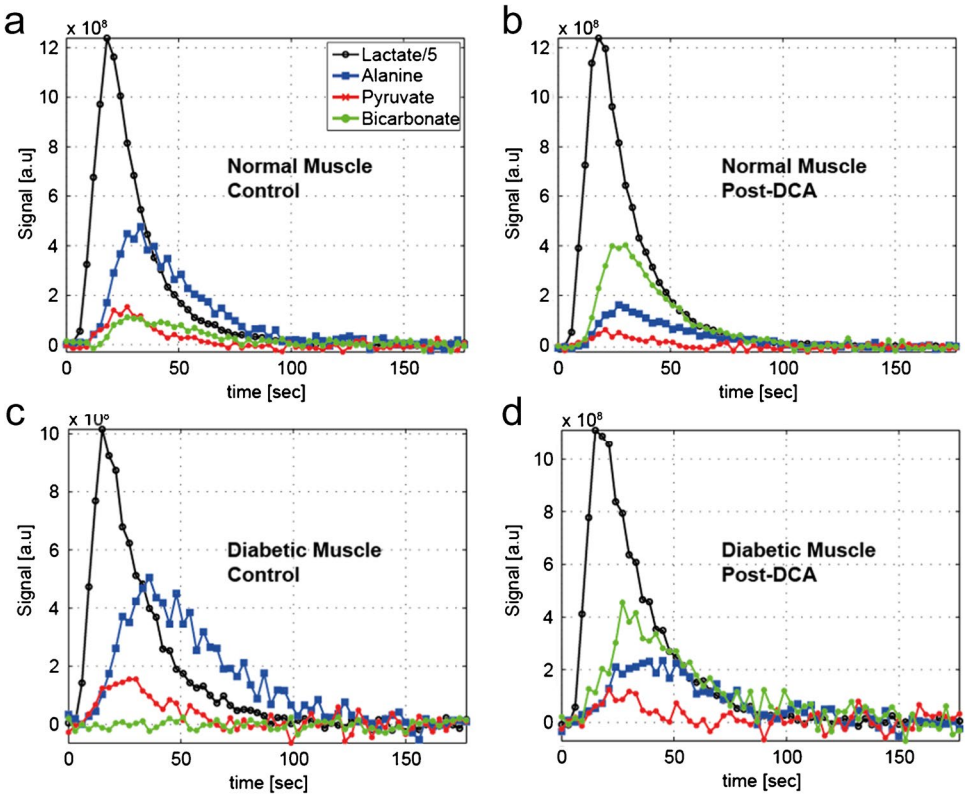

Fig. 2 Kinetics of individual metabolite from representative healthy and diabetic rat leg muscle after an injection of 40-mM hyperpolarized [1-^{13}C] lactate. (a) Normal muscle control, (b) normal muscle post-DCA, (c) diabetic muscle control, and (d) diabetic muscle post-DCA

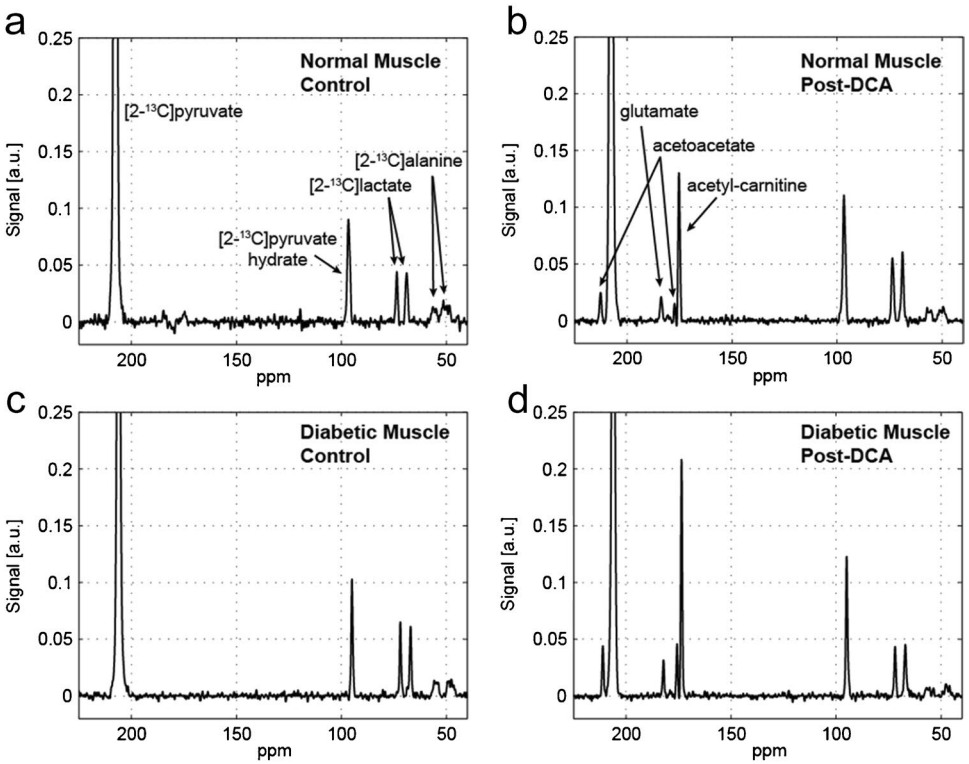

Fig. 3 Time-averaged spectra from representative healthy and diabetic rat leg muscle after an injection of 80-mM hyperpolarized [2-^{13}C]pyruvate. (a) Normal muscle control, (b) normal muscle post-DCA, (c) diabetic muscle control, and (d) diabetic muscle post-DCA

At baseline condition without DCA, dynamic analysis could not track mitochondrial metabolism based on the signals of ALCAR, AcAc, and glutamate (Fig. 4). Other relative metabolic production rates (r) and time-to-half maximum (τ) from the measured dynamic time-courses with and without DCA showed no significant difference between control and T2DM muscle (Table 2). Specifically, $\tau_{pyr\rightarrow lac}$ and $r_{pyr\rightarrow lac}$ exhibited similar values in pre-/post-DCA in CRL and T2DM muscle.

Histograms summarized the findings from [1-^{13}C]lactate and [2-^{13}C]pyruvate DNP experiments (Figs. 5 and 6). They compared the relative CRL and T2DM metabolite ratio and dynamic response to PDH activation with DCA.

Discussion

Pyruvate dehydrogenase kinetics of T2DM and healthy controls in vivo

The > 10,000 higher sensitivity of hyperpolarized molecules in the DNP NMR experiment provides a unique opportunity to measure PDH kinetics in vivo [1]. Studies have already demonstrated the method's utility in measuring metabolism kinetics in vivo with a 3-s temporal resolution [2, 40]. In these experiments, the time-averaged total carbon signal (tC) in the ^{13}C spectra serves as a normalization constant.

Integrated over 2 min in control muscle, the precursor lactate signal comprises 0.812 of the total ^{13}C signal in the spectra. LDH transfers 0.028 of tC to pyruvate. Alanine aminotransferase (ALT) catalyzes the conversion of pyruvate to alanine (0.129). Previous DNP experiments have confirmed that LDH can catalyze readily the conversion of from lactate to pyruvate in muscle, which provides a better window into the label distribution into alanine pool [4, 8, 40]. The apparent higher ^{13}C label flow from lactate into alanine than from lactate into pyruvate reflects a larger endogenous alanine pool. It does not necessarily indicate that ALT has a higher activity than LDH. Since myocytes contain 1.3–1.5 mM of endogenous ^{12}C-alanine and only 0.1 mM ^{12}C-pyruvate, the non-steady state ^{13}C exchange between alanine and pyruvate can initially increase the ^{13}C labeling of the alanine pool faster than the pyruvate pool. As a result, a higher signal intensity and apparent higher conversion rate to ^{13}C-alanine will appear.

In T2DM muscle, the precursor [1-^{13}C]lactate signal also comprises 0.821 of measured carbon signal. LDH in T2DM muscle converts comparable amount of lactate to pyruvate (0.026). However, ALT catalyzes a larger conversion to alanine (0.153). Instead of an alanine/pyruvate of 4.4 in healthy control muscle, T2DM shifts the ratio to 5.8. The increased conversion of lactate to alanine in T2DM muscle matches a reduced PDH activity. In previous studies, the analysis only determines the V_{PDH}/V_{TCA}

Table 2 Hyperpolarized [2-^{13}C] pyruvate metabolite distribution in control and T2DM rat leg muscle

	Baseline, No DCA		Post-DCA	
	Control	T2DM	Control	T2DM
Metabolite/total carbon				
Lactate/tC	0.040 ± 0.006	0.060 ± 0.003	0.046 ± 0.011	0.041 ± 0.009
Pyruvate/tC	0.854 ± 0.003	0.851 ± 0.018	0.808 ± 0.027	0.762 ± 0.031
Pyruvate-hydrate/tC	0.085 ± 0.011	0.075 ± 0.004	0.068 ± 0.002	0.070 ± 0.004
Alanine/tC	0.016 ± 0.008	0.008 ± 0.006	0.007 ± 0.004	0.008 ± 0.004
ALCAR/tC	N.D	N.D	0.044 ± 0.007	0.079 ± 0.009
AcAc/tC	N.D	N.D	0.018 ± 0.004	0.037 ± 0.004
Glutamate/tC	N.D	N.D	0.011 ± 0.001	0.010 ± 0.002
Metabolite ratio				
Lactate/pyruvate	0.047	0.071	0.057	0.054
Alanine/pyruvate	0.019	0.009	0.009	0.011
ALCAR/pyruvate	N.D	N.D	0.055	0.104
AcAc/pyruvate	N.D	N.D	0.022	0.049
Alanine/lactate	0.400	0.133	0.152	0.195
Relative metabolite production rate				
$r_{pyr\rightarrow lac}$	0.103 ± 0.032	0.128 ± 0.008	0.086 ± 0.022	0.130 ± 0.008
$r_{pyr\rightarrow ala}$	N.D	N.D	N.D	N.D
$r_{pyr\rightarrow pyh}$	0.111 ± 0.020	0.188 ± 0.050	0.148 ± 0.020	0.234 ± 0.022
$r_{pyr\rightarrow alcar}$	N.D	N.D	0.046 ± 0.011	0.053 ± 0.019
$r_{pyr\rightarrow acac}$	N.D	N.D	N.D	N.D
$r_{pyr\rightarrow glu}$	N.D	N.D	0.004 ± 0.003	0.024 ± 0.007
Time to half maximum [s]				
$\tau_{pyr\rightarrow lac}$	14.9 ± 1.2	12.1 ± 0.9	10.4 ± 0.4	12.8 ± 1.2
$\tau_{pyr\rightarrow ala}$	N.D	N.D	N.D	N.D
$\tau_{pyr\rightarrow pyh}$	9.9 ± 1.2	9.9 ± 0.2	7.8 ± 0.9	9.7 ± 0.8
$\tau_{pyr\rightarrow alcar}$	N.D	N.D	14.0 ± 0.9	14.7 ± 1.0
$\tau_{pyr\rightarrow acac}$	N.D	N.D	N.D	N.D
$\tau_{pyr\rightarrow glu}$	N.D	N.D	13.6 ± 0.9	14.7 ± 0.8

N.D., not detected

Statistically significant unpaired *t*-test ($P \leq 0.05$) and power ≥ 0.8:

Control v T2DM: Lac; Control-DCA v T2DM-DCA: ALCAR, AcAc, $r_{pyr\rightarrow pyh}$

ratio derived from ^{13}C alanine and glutamate fractional enrichment [58]. No measurement has tracked directly the V_{PDH} kinetics in vivo.

DNP NMR can directly measure the pyruvate decarboxylation reaction catalyzed by PDH. The kinetics confirms the decreased PDH activity in T2DM muscle. Given the unidirectional flux from pyruvate to HCO_3^-, exchange has no significant contribution in the analysis [12, 25]. In healthy muscle, PDH converts [1-^{13}C]lactate to 0.012 HCO_3^-/tC to yield a HCO_3^-/pyruvate ratio of 0.429. In T2DM muscle, PDH converts only 0.002 of the tC to HCO_3^- and yields a HCO_3^-/pyruvate ratio of 0.007. The HCO_3^-/pyruvate ratio of in control and diabetic muscle differs by a factor of 0.429/0.077 = 5.571. The observation agrees with DNP experiment finding in a study with streptozotocin induced diabetic heart [29]. T2DM lowers normal PDH activity by a factor of about 6.

Dichloroacetate and PDH Activation in healthy and T2DM muscle

If the reduced V_{PDH} originates from PDK activity, then a PDK inhibitor, such as DCA, can restore the PDH activity [62]. In both CRL and T2DM muscle, DCA addition does not alter the precursor lactate pool. Instead, it increases pyruvate to HCO_3^- flux and decreases pyruvate and alanine levels. In CRL muscle, DCA induces HCO_3^-/tC to increase from 0.012 to 0.076, 6.3 times above the control level. Pyruvate/tC drops precipitously from 0.028 to 0.009 and alanine/tC decreases from 0.129 to 0.050. In the presence of DCA, PDH competes immediately with the near equilibrium LDH and ALT for pyruvate [17]. It does not exhibit any metabolic inertia as some researchers have hypothesized [13, 67].

In T2DM muscle, DCA induces an even more marked change in PDH activity. Without DCA, T2DM muscle

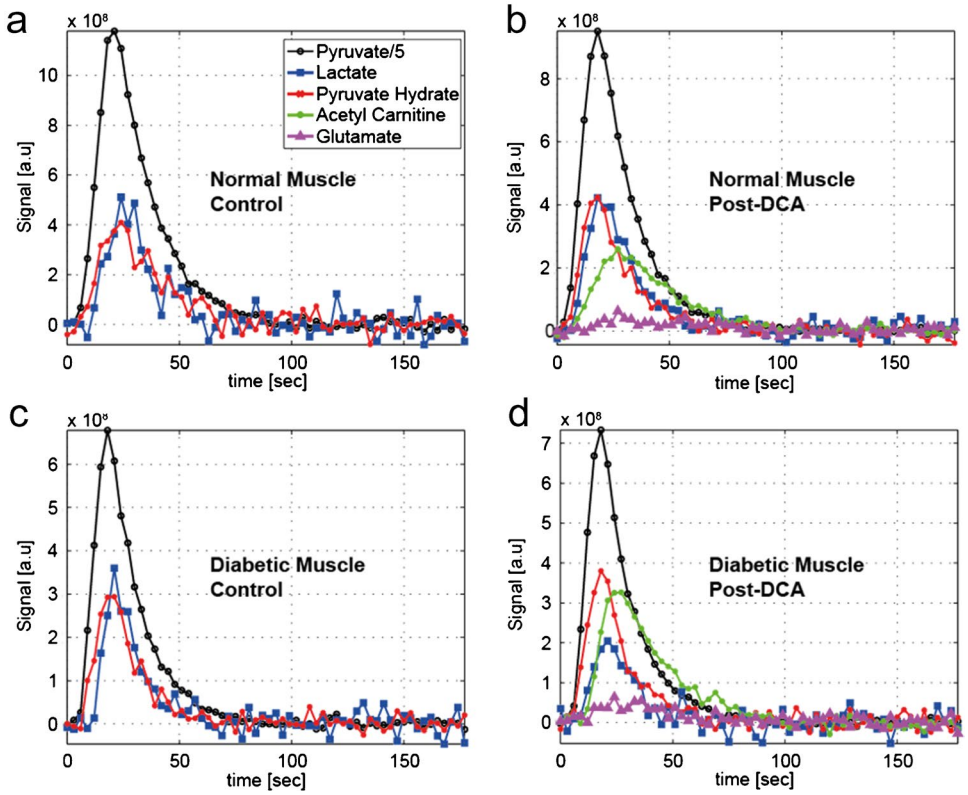

Fig. 4 Kinetics of individual metabolite from representative healthy and diabetic rat leg muscle after an injection of 80-mM hyperpolarized [2-^{13}C] pyruvate. (a) Normal muscle control, (b) normal muscle post-DCA, (c) diabetic muscle control, and (d) diabetic muscle post-DCA

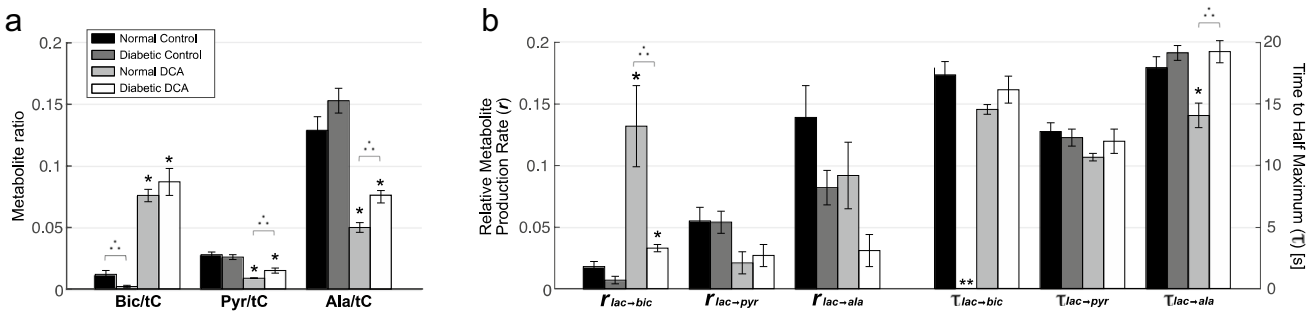

Fig. 5 Histogram of DCA effects on control and T2DM rat leg muscle measured with 40-mM hyperpolarized [1-^{13}C]lactate. (a) Metabolite ratio and (b) dynamic analysis. "*" indicates statistically significant difference between control and post-DCA measurements. "**" indicates that the metabolite was not detected. "∴" indicates statistically significant difference between normal and diabetic muscle measurements

produces almost 6 times less HCO_3^-/tC from [1-^{13}C]lactate than control muscle, 0.002 vs. 0.012. However, DCA activates both CRL and T2DM muscle to produce a comparable amount of HCO_3^-/tC: T2DM, 0.087/tC; CRL, 0.076/tC. Because the resting PDH activities in T2DM and CRL muscle differ so markedly (0.012 vs 0.002), DCA induces a much larger dynamic change in the PDH activity in T2DM muscle (0.087/0.002 = 43.5) than in CRL muscle (0.076/0.012 = 6.3). The contrasting shift in PDH activity (43.5/6.3 = 6.9 times) arises from the reduced PDH activity in resting T2DM muscle. Diabetes suppresses PDH activity, but DCA can fully activate it to the same level.

Even though DCA restores the PDH activity in T2DM to produce the equivalent amount of HCO_3^-/tC within the 2-min experiment period, the enzyme kinetics profiles do not share the same mechanistic paths. In CRL muscle, DCA induces a relative reaction rate, $r_{lac\rightarrow bic}$, of 0.132, whereas in T2DM muscle, it induces a rate of 0.033. The PDH kinetics in T2DM responds initially 4 times slower to DCA than the

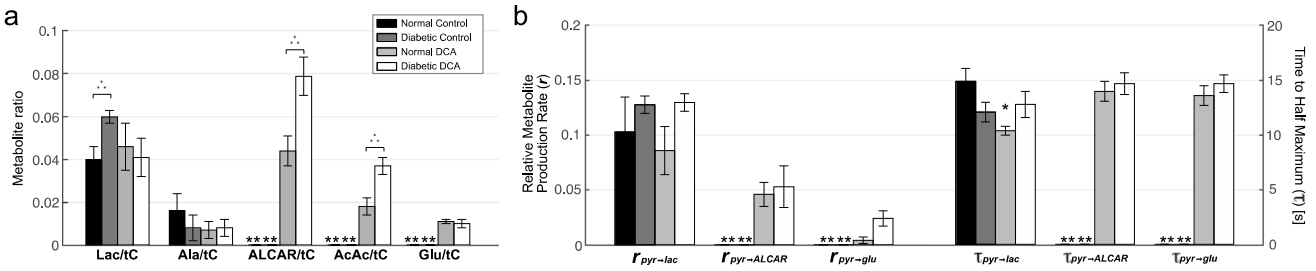

Fig. 6 Histogram of DCA effects on control and T2DM rat leg muscle measured by 80-mM hyperpolarized [2-^{13}C]pyruvate. (a) Metabolite ratio and (b) dynamic analysis. "*" indicates statistically significant difference between control and post-DCA measurements. "**" indicates that the metabolite was not detected. "∴" indicates statistically significant difference between normal and diabetic muscle measurements

PDH in control muscle. At present, the slower mechanism remains unclear and may involve the interaction of different PDKs that contribute to the overall PDH impairment in T2DM [7].

Acetyl carnitine

Injecting [2-^{13}C]pyruvate as the precursor confirms the depressed PDH activity in T2DM and has also mapped the ALCAR and TCA fluxes. Control and diabetic muscles yield a similar pyr/tC, 0.854 and 0.851, respectively. However, T2DM muscle increases pyruvate to lactate conversion from 0.040 to 0.060. In T2DM muscle, lactate/pyruvate increases from 0.047 to 0.071. The increasing lactate/pyruvate ratio agrees with a reduced PDH activity. Unfortunately, the poor signal-to-noise ratio precludes using the alanine signal in the analysis.

In contrast to [1-^{13}C]lactate experiments, the [2-^{13}C] pyruvate experiments can follow PDH flux into ALCAR in resting muscle. However, DNP does not presently have sufficient sensitivity to detect the ALCAR signal in either CRL or T2DM resting muscle. However, given the limit of detection estimated from the lowest detectable HCO_3^-/tC signal (0.002), the ALCAR level must fall well below 0.002.

Upon DCA activation, PDH converts rapidly pyruvate to ALCAR (ALCAR/tC = 0.044) in CRL and 0.079 in and T2DM. T2DM has a 1.79 (0.079/0.044) × higher conversion of pyruvate to ALCAR than CRL muscle. Consistent with the increased flux into the acetyl CoA pool, AcAc level increases to 0.018 in CRL muscle and to 0.037 in T2DM muscle. Assuming an equivalent CRL and T2DM ALCAR in the resting state yields a lower estimate of the relative DCA induced PDH change in T2DM/CRL, 0.079/0.044 = 1.79. Since [1-^{13}C]lactate produces 6 times less HCO_3^- in T2DM than in CRL muscle, the T2DM ALCAR pool could stand correspondingly 6 times lower. Using a lower estimate of the resting ALCAR pool in T2DM would enlarge the relative change in PDH activity in T2DM/CRL from 1.79 to 10.8 times.

The differential ALCAR/tC signal does not arise from a larger endogenous ALCAR pool in diabetic muscle, which could enhance the distribution of ^{13}C label in the ALCAR pool. The increased AcAc pool would militate against such an interpretation. Moreover, in vivo NMR experiments have determined that T2DM muscle has a lower ALCAR level than CRL muscle [30]. The increase in the ALCAR signal upon DCA activation appears to correspond to an increased flux into ALCAR.

The rapid production of ALCAR with DCA activation of PDH argues against a diminished expression of CrAT and for an altered CrAT equilibrium to account for the diminished ALCAR pool in the resting T2DM muscle. A diminished ALCAR pool, however, does not provide any evidence for an enlarged acetyl CoA in resting T2DM, which would serve to inhibit resting PDH activity as envisioned in elements of the Randle cycle model [18].

Impairment in TCA and electron transport chain

A lower PDH activity alone cannot explain fully the metabolic dysregulation observed in T2DM, since previous studies have observed a decrease in the oxidative enzyme levels and activities in T2DM muscle [14, 27, 37, 44, 60, 68]. Indeed, the activity of rotenone-sensitive NADH:O_2 oxidoreductase and citrate synthase decreases by 40% in muscle from T2DM patients, and transmission electron microscopy reveals reduced mitochondrial size and altered morphology [22]. Gene expression also detects a decrease in oxidative phosphorylation enzymes [35, 41]. Some studies have also detected altered mitochondrial activity in T2DM [60]. However, not all studies have observed an abnormal mitochondrial function and a reduced ATP turnover in age-matched control T2DM muscle [6, 34, 65].

NMR experiments have also observed impairments in TCA and oxidative phosphorylation. ^{13}C-acetate incorporates into glutamate at a lower rate than control muscle, which reflects a decreased V_{TCA}. ^{31}P saturation transfer measurements reveal a lower ATP turnover, consistent with

a lower oxidative phosphorylation efficiency [5, 43, 45, 46]. Even insulin-resistant offspring of parents with T2DM exhibit a 30% decrease in ATP synthesis and a lower ATP turnover to O_2 consumption (P/O) ratio as determined by NMR saturation transfer and glutamate kinetics experiments [42, 44]. Even though some investigators have raised concerns about the accuracy of the saturation transfer method to determine exclusively the mitochondrial ATP turnover rate and the use of glutamate turnover to estimate accurately the O_2 consumption, the results, nevertheless, indicate that activating PDH alone might not increase TCA activity, oxidative phosphorylation, and insulin sensitivity [24].

Indeed, the DNP experiment confirms such a viewpoint. Without DCA, NMR cannot detect any [5-^{13}C]glutamate signal. With DCA, however, NMR can now assess the [5-^{13}C]glutamate signals in CRL and T2DM muscle. Since α-ketoglutarate stands in near equilibrium with glutamate, the [5-^{13}C]glutamate signal reflects the TCA flux (V_{TCA}). In many metabolic models, V_{PDH} constitutes a rate limiting step for acetyl CoA formation and V_{TCA} [50, 58]. V_{TCA} should match proportionately the change in V_{PDH}.

Because DCA enhances the PDH flux in T2DM much more than in CRL, the surge in the T2DM acetyl CoA and ALCAR should exceed the corresponding change in CRL. Yet, the differential surge in V_{PDH} does not produce any contrasting change in V_{TCA}. DCA stimulation of PDH activity produces the same level of [5-^{13}C]glutamate in CRL and T2DM muscle. The results suggest that V_{TCA} does not always match V_{PDH} in the same proportion and that the equilibration between acetyl CoA and ALCAR can buffer acetyl CoA availability. The mismatched V_{TCA} and V_{PDH} during DCA addition may also point to downstream impairments in ETC, respiration, and oxidative phosphorylation in T2DM, which can arise from a reduction of AMP-activated protein kinase activity or from an altered recycling of the NAD^+/NADH pool through the glycerophosphate dehydrogenase shuttle [31, 32, 70].

PDK inhibition in T2DM

Inhibiting PDK may then have limited impact on improving oxidative phosphorylation and insulin resistance in T2DM muscle [33, 63]. Experiments with a PDK2 and PDK4 double knock-out (DKO)mouse model show enhanced glucose oxidation but still insulin resistance [50]. V_{TCA} remains invariant in the DNP experiments, even though DCA induces a differential rise in V_{PDH} in CRL and T2DM muscle. The results suggest that the ALCAR reaction has buffered the available acetyl CoA for TCA, and a downstream ETC activity limits the impact of an increasing level of acetyl CoA on the V_{TCA}.

Even though in vivo ^{13}C study of human T2DM muscle has established that non-oxidative metabolism, such as glycogen synthesis, can account for the reduced glucose delivery/metabolism in T2DM, linking impaired oxidative metabolism to insulin resistance continues to pose the critical question. The lower mitochondria population and activity could certainly decrease the fatty acid oxidation capacity, despite elevated levels of plasma fatty acid and intramyocellular lipid (IMCL) [20]35, 41. Indeed, an alternative hypothesis to the Randle cycle has envisioned insufficient β-oxidation contributing to tissue accumulation of lipids, which would increase IMCL, such as acyl glycerol intermediates. The acyl glycerol intermediates can directly diminish the insulin receptor substrate 1 (IRS-1) and reduce the release of glucose transporters 4 (GLUT4) from vesicles [15, 47, 54]. In diabetic rodent, insulin resistance correlates with the accumulation of acylcarnitine [28]. However, in vivo NMR detects a decreased level ALCAR in T2DM human muscle [30].

Since the acetyl CoA to ALCAR reaction catalyzed by CrAT has an equilibrium constant of 1.6 at 25 °C, the much lower HCO_3^-/tC signal in the T2DM vs CRL implies that diabetic cell has both decreased levels of acetyl CoA and ALCAR, consistent with insufficient β-oxidation [48]. Upon DCA stimulation of PDH, CrAT immediately catalyzes the formation ALCAR to buffer the surge in acetyl CoA. Given the observed accumulated acylcarnitine in diabetic muscle, a shift in the acylcarnitine-carnitine equilibrium must accompany the rapid ALCAR formation during DCA inhibition of PDK. Such an interpretation suggests CrAT buffers both acetyl CoA and carnitine availability. Indeed, dietary L-carnitine supplementation appears to rescue the muscle from a metabolic flexibility [23, 36, 49]. However, substantiating the role of CrAT in controlling insulin resistance requires further study.

Conclusion

T2DM rat muscle has a much lower resting PDH activity than control muscle, based on hyperpolarized [1-^{13}C]lactate experiments. [2-^{13}C]Pyruvate experiments have confirmed the interpretation. With DCA, PDH activity in T2DM recovers quickly to CRL level. Even though DCA increases the PDH flux from pyruvate to acetyl CoA, V_{TCA}, as reflected in [5-^{13}C]glutamate signal, does not match the differential surge in V_{PDH}. The mismatch between V_{PDH} and V_{TCA} muscle during DCA activation suggests that T2DM muscle has impairments in ETC and oxidative phosphorylation or an altered CrAT equilibrium. Consequently, using PDK inhibition to activate PDH may not restore oxidative phosphorylation or insulin sensitivity in T2DM muscle. The study has applied DNP NMR to a unique T2DM rodent model to gain insight into the biochemical mechanism underlying the control of PDH activity.

Author contribution JMP, REH, DM, DMS, and TJ contributed to the conception and design of research; JMP, SJ, REH, JG, DB, and TJ performed experiments; JMP, SJ, REH, JG, PH, DB, DM, YC, DMS, and TJ discussed, analyzed, and interpreted experiment data; JMP and TJ prepared figures, analyzed the data, wrote the drafts of the manuscript, and incorporated comments; JMP, SJ, REH, JG, PH, DB, DM, YC, DMS, and TJ reviewed and approved the final version of the manuscript.

Funding The study acknowledges funding support from the National Institutes of Health (NIH) CA176836, AA005965, AA018681, S10 OD012283, P41 EB015891 (DS); the US Department of Defense PC100427 (DS); NIH EB009070, DK106395, NS096575, CA213020 (DM); NIH R01NS107409 (JMP); the Welch Foundation I-2009–20190330 (JMP); DK095960, DK087307 (PH); the France-Berkeley Fund (TJ & DB); and California Department of Public Health 18–10923 (TJ).

Availability of data and material All data generated or analyzed during this study are included in this published article.

Declarations

Ethics approval Animal care and experimental procedures followed the guidelines of the National Institute of Health Office for Laboratory Animal Welfare and were approved by the local Institutional Animal Care and Use Committee.

Conflict of interest The authors declare no competing interest.

References

1. Ardenkjaer-Larsen JH, Fridlund B, Gram A, Hansson G, Hansson L, Lerche MH, Servin R, Thaning M, Golman K (2003) Increase in signal-to-noise ratio of > 10,000 times in liquid-state NMR. Proc Natl Acad Sci U S A 100:10158–10163. https://doi.org/10.1073/pnas.1733835100
2. Atherton HJ, Schroeder MA, Dodd MS, Heather LC, Carter EE, Cochlin LE, Nagel S, Sibson NR, Radda GK, Clarke K, Tyler DJ (2011) Validation of the in vivo assessment of pyruvate dehydrogenase activity using hyperpolarised 13C MRS. NMR Biomed 24:201–208. https://doi.org/10.1002/nbm.1573
3. Backshear PJ, Holloway PA, Alberti KG (1975) Metabolic interactions of dichloroacetate and insulin in experimental diabetic ketoacidosis. Biochem J 146:447–456. https://doi.org/10.1042/bj1460447
4. Bastiaansen JAM, Yoshihara HAL, Takado Y, Gruetter R, Comment A (2014) Hyperpolarized ^{13}C lactate as a substrate for in vivo metabolic studies in skeletal muscle. Metabolomics 10:986–994. https://doi.org/10.1007/s11306-014-0630-5
5. Befroy DE, Petersen KF, Dufour S, Mason GF, de Graaf RA, Rothman DL, Shulman GI (2007) Impaired mitochondrial substrate oxidation in muscle of insulin-resistant offspring of type 2 diabetic patients. Diabetes 56:1376–1381. https://doi.org/10.2337/db06-0783
6. Boushel R, Gnaiger E, Schjerling P, Skovbro M, Kraunsoe R, Dela F (2007) Patients with type 2 diabetes have normal mitochondrial function in skeletal muscle. Diabetologia 50:790–796. https://doi.org/10.1007/s00125-007-0594-3
7. Bowker-Kinley MM, Davis WI, Wu P, Harris RA, Popov KM (1998) Evidence for existence of tissue-specific regulation of the mammalian pyruvate dehydrogenase complex. Biochem J 329(Pt 1):191–196. https://doi.org/10.1042/bj3290191
8. Brooks GA (2009) Cell-cell and intracellular lactate shuttles. J Physiol 587:5591–5600. https://doi.org/10.1113/jphysiol.2009.178350
9. Cline GW, Lepine RL, Papas KK, Kibbey RG, Shulman GI (2004) 13C NMR isotopomer analysis of anaplerotic pathways in INS-1 cells. J Biol Chem 279:44370–44375. https://doi.org/10.1074/jbc.M311842200
10. Cummings BP, Bettaieb A, Graham JL, Stanhope KL, Dill R, Morton GJ, Haj FG, Havel PJ (2011) Subcutaneous administration of leptin normalizes fasting plasma glucose in obese type 2 diabetic UCD-T2DM rats. Proc Natl Acad Sci U S A 108:14670–14675. https://doi.org/10.1073/pnas.1107163108
11. Cummings BP, Digitale EK, Stanhope KL, Graham JL, Baskin DG, Reed BJ, Sweet IR, Griffen SC, Havel PJ (2008) Development and characterization of a novel rat model of type 2 diabetes mellitus: the UC Davis type 2 diabetes mellitus UCD-T2DM rat. Am J Physiol Regul Integr Comp Physiol 295:R1782–R1793. https://doi.org/10.1152/ajpregu.90635.2008
12. Day SE, Kettunen MI, Gallagher FA, Hu DE, Lerche M, Wolber J, Golman K, Ardenkjaer-Larsen JH, Brindle KM (2007) Detecting tumor response to treatment using hyperpolarized 13C magnetic resonance imaging and spectroscopy. Nat Med 13:1382–1387. https://doi.org/10.1038/nm1650
13. Grassi B, Gladden LB, Samaja M, Stary CM, Hogan MC (1998) Faster adjustment of O2 delivery does not affect V(O2) on-kinetics in isolated in situ canine muscle. J Appl Physiol 85:1394–1403. https://doi.org/10.1152/jappl.1998.85.4.1394
14. He J, Watkins S, Kelley DE (2001) Skeletal muscle lipid content and oxidative enzyme activity in relation to muscle fiber type in type 2 diabetes and obesity. Diabetes 50:817–823
15. Hesselink MK, Schrauwen-Hinderling V, Schrauwen P (2016) Skeletal muscle mitochondria as a target to prevent or treat type 2 diabetes mellitus. Nat Rev Endocrinol 12:633–645. https://doi.org/10.1038/nrendo.2016.104
16. Holness MJ, Kraus A, Harris RA, Sugden MC (2000) Targeted upregulation of pyruvate dehydrogenase kinase (PDK)-4 in slow-twitch skeletal muscle underlies the stable modification of the regulatory characteristics of PDK induced by high-fat feeding. Diabetes 49:775–781. https://doi.org/10.2337/diabetes.49.5.775
17. Howlett RA, Heigenhauser GJ, Hultman E, Hollidge-Horvat MG, Spriet LL (1999) Effects of dichloroacetate infusion on human skeletal muscle metabolism at the onset of exercise. Am J Physiol 277:E18–E25
18. Hue L, Taegtmeyer H (2009) The Randle cycle revisited: a new head for an old hat. Am J Physiol Endocrinol Metab 297:E578-591. https://doi.org/10.1152/ajpendo.00093.2009
19. Jeoung NH, Harris RA (2008) Pyruvate dehydrogenase kinase-4 deficiency lowers blood glucose and improves glucose tolerance in diet-induced obese mice. Am J Physiol Endocrinol Metab 295:E46-54. https://doi.org/10.1152/ajpendo.00536.2007
20. Kautzky-Willer A, Krssak M, Winzer C, Pacini G, Tura A, Farhan S, Wagner O, Brabant G, Horn R, Stingl H, Schneider B, Waldhausl W, Roden M (2003) Increased intramyocellular lipid concentration identifies impaired glucose metabolism in women with previous gestational diabetes. Diabetes 52:244–251
21. Kelley DE, Goodpaster BH, Storlien L (2002) Muscle triglyceride and insulin resistance. Annu Rev Nutr 22:325–346. https://doi.org/10.1146/annurev.nutr.22.010402.102912
22. Kelley DE, He J, Menshikova EV, Ritov VB (2002) Dysfunction of mitochondria in human skeletal muscle in type 2 diabetes. Diabetes 51:2944–2950. https://doi.org/10.2337/diabetes.51.10.2944

23. Kelley DE, Mandarino LJ (2000) Fuel selection in human skeletal muscle in insulin resistance: a reexamination. Diabetes 49:677–683. https://doi.org/10.2337/diabetes.49.5.677
24. Kemp GJ, Brindle KM (2012) What do magnetic resonance-based measurements of Pi–>ATP flux tell us about skeletal muscle metabolism? Diabetes 61:1927–1934. https://doi.org/10.2337/db11-1725
25. Kettunen MI, Hu DE, Witney TH, McLaughlin R, Gallagher FA, Bohndiek SE, Day SE, Brindle KM (2010) Magnetization transfer measurements of exchange between hyperpolarized [1-13C] pyruvate and [1-13C]lactate in a murine lymphoma. Magn Reson Med 63:872–880. https://doi.org/10.1002/mrm.22276
26. Kleinert M, Clemmensen C, Hofmann SM, Moore MC, Renner S, Woods SC, Huypens P, Beckers J, de Angelis MH, Schurmann A, Bakhti M, Klingenspor M, Heiman M, Cherrington AD, Ristow M, Lickert H, Wolf E, Havel PJ, Muller TD, Tschop MH (2018) Animal models of obesity and diabetes mellitus. Nat Rev Endocrinol 14:140–162. https://doi.org/10.1038/nrendo.2017.161
27. Koliaki C, Roden M (2016) Alterations of mitochondrial function and insulin sensitivity in human obesity and diabetes mellitus. Annu Rev Nutr 36:337–367. https://doi.org/10.1146/annurev-nutr-071715-050656
28. Koves TR, Ussher JR, Noland RC, Slentz D, Mosedale M, Ilkayeva O, Bain J, Stevens R, Dyck JR, Newgard CB, Lopaschuk GD, Muoio DM (2008) Mitochondrial overload and incomplete fatty acid oxidation contribute to skeletal muscle insulin resistance. Cell Metab 7:45–56. https://doi.org/10.1016/j.cmet.2007.10.013
29. Le Page LM, Rider OJ, Lewis AJ, Ball V, Clarke K, Johansson E, Carr CA, Heather LC, Tyler DJ (2015) Increasing pyruvate dehydrogenase flux as a treatment for diabetic cardiomyopathy: a combined 13C hyperpolarized magnetic resonance and echocardiography study. Diabetes 64:2735–2743. https://doi.org/10.2337/db14-1560
30. Lindeboom L, Nabuurs CI, Hoeks J, Brouwers B, Phielix E, Kooi ME, Hesselink MK, Wildberger JE, Stevens RD, Koves T, Muoio DM, Schrauwen P, Schrauwen-Hinderling VB (2014) Long-echo time MR spectroscopy for skeletal muscle acetylcarnitine detection. J Clin Invest 124:4915–4925. https://doi.org/10.1172/JCI74830
31. Madiraju AK, Erion DM, Rahimi Y, Zhang XM, Braddock DT, Albright RA, Prigaro BJ, Wood JL, Bhanot S, MacDonald MJ, Jurczak MJ, Camporez JP, Lee HY, Cline GW, Samuel VT, Kibbey RG, Shulman GI (2014) Metformin suppresses gluconeogenesis by inhibiting mitochondrial glycerophosphate dehydrogenase. Nature 510:542–546. https://doi.org/10.1038/nature13270
32. Madiraju AK, Qiu Y, Perry RJ, Rahimi Y, Zhang XM, Zhang D, Camporez JG, Cline GW, Butrico GM, Kemp BE, Casals G, Steinberg GR, Vatner DF, Petersen KF, Shulman GI (2018) Metformin inhibits gluconeogenesis via a redox-dependent mechanism in vivo. Nat Med 24:1384–1394. https://doi.org/10.1038/s41591-018-0125-4
33. Mayers RM, Leighton B, Kilgour E (2005) PDH kinase inhibitors: a novel therapy for Type II diabetes? Biochem Soc Trans 33:367–370. https://doi.org/10.1042/BST0330367
34. Mogensen M, Sahlin K, Fernstrom M, Glintborg D, Vind BF, Beck-Nielsen H, Hojlund K (2007) Mitochondrial respiration is decreased in skeletal muscle of patients with type 2 diabetes. Diabetes 56:1592–1599. https://doi.org/10.2337/db06-0981
35. Mootha VK, Lindgren CM, Eriksson KF, Subramanian A, Sihag S, Lehar J, Puigserver P, Carlsson E, Ridderstrale M, Laurila E, Houstis N, Daly MJ, Patterson N, Mesirov JP, Golub TR, Tamayo P, Spiegelman B, Lander ES, Hirschhorn JN, Altshuler D, Groop LC (2003) PGC-1alpha-responsive genes involved in oxidative phosphorylation are coordinately downregulated in human diabetes. Nat Genet 34:267–273. https://doi.org/10.1038/ng1180
36. Noland RC, Koves TR, Seiler SE, Lum H, Lust RM, Ilkayeva O, Stevens RD, Hegardt FG, Muoio DM (2009) Carnitine insufficiency caused by aging and overnutrition compromises mitochondrial performance and metabolic control. J Biol Chem 284:22840–22852. https://doi.org/10.1074/jbc.M109.032888
37. Ortenblad N, Mogensen M, Petersen I, Hojlund K, Levin K, Sahlin K, Beck-Nielsen H, Gaster M (2005) Reduced insulin-mediated citrate synthase activity in cultured skeletal muscle cells from patients with type 2 diabetes: evidence for an intrinsic oxidative enzyme defect. Biochim Biophys Acta 1741:206–214. https://doi.org/10.1016/j.bbadis.2005.04.001
38. Park JM, Harrison CE, Ma J, Chen J, Ratnakar J, Zun Z, Liticker J, Reed GD, Chhabra A, Haller RG, Jue T, Malloy CR (2021) Hyperpolarized (13)C MR spectroscopy depicts in vivo effect of exercise on pyruvate metabolism in human skeletal muscle. Radiology:204500. https://doi.org/10.1148/radiol.2021204500
39. Park JM, Josan S, Mayer D, Hurd R, Spielman D, Bendahan D, Jue T (2013) Direct observation of lactate metabolsim in skeletal muscle with hyperpolarized 13C NMR. World Molecular Imaging Congress:LBA 9
40. Park JM, Josan S, Mayer D, Hurd RE, Chung Y, Bendahan D, Spielman DM, Jue T (2015) Hyperpolarized 13C NMR observation of lactate kinetics in skeletal muscle. J Exp Biol 218:3308–3318. https://doi.org/10.1242/jeb.123141
41. Patti ME, Butte AJ, Crunkhorn S, Cusi K, Berria R, Kashyap S, Miyazaki Y, Kohane I, Costello M, Saccone R, Landaker EJ, Goldfine AB, Mun E, DeFronzo R, Finlayson J, Kahn CR, Mandarino LJ (2003) Coordinated reduction of genes of oxidative metabolism in humans with insulin resistance and diabetes: potential role of PGC1 and NRF1. Proc Natl Acad Sci U S A 100:8466–8471. https://doi.org/10.1073/pnas.1032913100
42. Patti ME, Corvera S (2010) The role of mitochondria in the pathogenesis of type 2 diabetes. Endocr Rev 31:364–395. https://doi.org/10.1210/er.2009-0027
43. Petersen KF, Befroy D, Dufour S, Dziura J, Ariyan C, Rothman DL, DiPietro L, Cline GW, Shulman GI (2003) Mitochondrial dysfunction in the elderly: possible role in insulin resistance. Science 300:1140–1142. https://doi.org/10.1126/science.1082889
44. Petersen KF, Dufour S, Befroy D, Garcia R, Shulman GI (2004) Impaired mitochondrial activity in the insulin-resistant offspring of patients with type 2 diabetes. N Engl J Med 350:664–671. https://doi.org/10.1056/NEJMoa031314
45. Petersen KF, Dufour S, Shulman GI (2005) Decreased insulin-stimulated ATP synthesis and phosphate transport in muscle of insulin-resistant offspring of type 2 diabetic parents. PLoS Med 2:e233. https://doi.org/10.1371/journal.pmed.0020233
46. Petersen KF, Morino K, Alves TC, Kibbey RG, Dufour S, Sono S, Yoo PS, Cline GW, Shulman GI (2015) Effect of aging on muscle mitochondrial substrate utilization in humans. Proc Natl Acad Sci U S A 112:11330–11334. https://doi.org/10.1073/pnas.1514844112
47. Petersen MC, Shulman GI (2018) Mechanisms of insulin action and insulin resistance. Physiol Rev 98:2133–2223. https://doi.org/10.1152/physrev.00063.2017
48. Pieklik JR, Guynn RW (1975) Equilibrium constants of the reactions of choline acetyltransferase, carnitine acetyltransferase, and acetylcholinesterase under physiological conditions. J Biol Chem 250:4445–4450
49. Power RA, Hulver MW, Zhang JY, Dubois J, Marchand RM, Ilkayeva O, Muoio DM, Mynatt RL (2007) Carnitine revisited: potential use as adjunctive treatment in diabetes. Diabetologia 50:824–832. https://doi.org/10.1007/s00125-007-0605-4
50. Rahimi Y, Camporez JP, Petersen MC, Pesta D, Perry RJ, Jurczak MJ, Cline GW, Shulman GI (2014) Genetic activation of pyruvate dehydrogenase alters oxidative substrate selection to induce

skeletal muscle insulin resistance. Proc Natl Acad Sci U S A 111:16508–16513. https://doi.org/10.1073/pnas.1419104111
51. Randle PJ, Garland PB, Hales CN, Newsholme EA (1963) The glucose fatty-acid cycle. Its role in insulin sensitivity and the metabolic disturbances of diabetes mellitus. Lancet 1:785–789. https://doi.org/10.1016/s0140-6736(63)91500-9
52. Roden M, Price TB, Perseghin G, Petersen KF, Rothman DL, Cline GW, Shulman GI (1996) Mechanism of free fatty acid-induced insulin resistance in humans. J Clin Invest 97:2859–2865. https://doi.org/10.1172/JCI118742
53. Rothman DL, Shulman RG, Shulman GI (1992) 31P nuclear magnetic resonance measurements of muscle glucose-6-phosphate. Evidence for reduced insulin-dependent muscle glucose transport or phosphorylation activity in non-insulin-dependent diabetes mellitus. J Clin Invest 89:1069–1075. https://doi.org/10.1172/JCI115686
54. Samuel VT, Petersen KF, Shulman GI (2010) Lipid-induced insulin resistance: unravelling the mechanism. Lancet 375:2267–2277. https://doi.org/10.1016/S0140-6736(10)60408-4
55. Samuel VT, Shulman GI (2016) The pathogenesis of insulin resistance: integrating signaling pathways and substrate flux. J Clin Invest 126:12–22. https://doi.org/10.1172/JCI77812
56. Schroeder MA, Ali MA, Hulikova A, Supuran CT, Clarke K, Vaughan-Jones RD, Tyler DJ, Swietach P (2013) Extramitochondrial domain rich in carbonic anhydrase activity improves myocardial energetics. Proc Natl Acad Sci U S A 110:E958-967. https://doi.org/10.1073/pnas.1213471110
57. Schroeder MA, Cochlin LE, Heather LC, Clarke K, Radda GK, Tyler DJ (2008) In vivo assessment of pyruvate dehydrogenase flux in the heart using hyperpolarized carbon-13 magnetic resonance. Proc Natl Acad Sci U S A 105:12051–12056. https://doi.org/10.1073/pnas.0805953105
58. Shulman GI, Rossetti L, Rothman DL, Blair JB, Smith D (1987) Quantitative analysis of glycogen repletion by nuclear magnetic resonance spectroscopy in the conscious rat. J Clin Invest 80:387–393. https://doi.org/10.1172/JCI113084
59. Shulman GI, Rothman DL, Jue T, Stein P, DeFronzo RA, Shulman RG (1990) Quantitation of muscle glycogen synthesis in normal subjects and subjects with non-insulin-dependent diabetes by 13C nuclear magnetic resonance spectroscopy. N Engl J Med 322:223–228
60. Simoneau JA (1985) Kelley DE (1997) Altered glycolytic and oxidative capacities of skeletal muscle contribute to insulin resistance in NIDDM. J Appl Physiol 83:166–171. https://doi.org/10.1152/jappl.1997.83.1.166
61. Spriet LL, Heigenhauser GJ (2002) Regulation of pyruvate dehydrogenase (PDH) activity in human skeletal muscle during exercise. Exerc Sport Sci Rev 30:91–95. https://doi.org/10.1097/00003677-200204000-00009
62. Stacpoole PW (1989) The pharmacology of dichloroacetate. Metabolism 38:1124–1144. https://doi.org/10.1016/0026-0495(89)90051-6
63. Stacpoole PW, Moore GW, Kornhauser DM (1978) Metabolic effects of dichloroacetate in patients with diabetes mellitus and hyperlipoproteinemia. 298:526–530. https://doi.org/10.1016/0026-0495(89)90051-6
64. Sugden MC, Holness MJ, Palmer TN (1989) Fuel selection and carbon flux during the starved-to-fed transition. Biochem J 263:313–323. https://doi.org/10.1042/bj2630313
65. Szendroedi J, Schmid AI, Chmelik M, Toth C, Brehm A, Krssak M, Nowotny P, Wolzt M, Waldhausl W, Roden M (2007) Muscle mitochondrial ATP synthesis and glucose transport/phosphorylation in type 2 diabetes. PLoS Med 4:e154. https://doi.org/10.1371/journal.pmed.0040154
66. Timmons JA, Poucher SM, Constantin-Teodosiu D, Worrall V, Macdonald IA, Greenhaff PL (1996) Increased acetyl group availability enhances contractile function of canine skeletal muscle during ischemia. J Clin Invest 97:879–883. https://doi.org/10.1172/JCI118490
67. Tschakovsy ME, Hughson RL (1999) Interaction of factors determining oxygen uptake at the onset of exercise. J Appl 86:1101–1113. https://doi.org/10.1152/jappl.1999.86.4.1101
68. Vondra K, Rath R, Bass A, Slabochova Z, Teisinger J, Vitek V (1977) Enzyme activities in quadriceps femoris muscle of obese diabetic male patients. Diabetologia 13:527–529. https://doi.org/10.1007/BF01234508
69. Zhang S, Hulver MW, McMillan RP, Cline MA, Gilbert ER (2014) The pivotal role of pyruvate dehydrogenase kinases in metabolic flexibility. Nutr Metab (Lond) 11:10. https://doi.org/10.1186/1743-7075-11-10
70. Zhou G, Myers R, Li Y, Chen Y, Shen X, Fenyk-Melody J, Wu M, Ventre J, Doebber T, Fujii N, Musi N, Hirshman MF, Goodyear LJ, Moller DE (2001) Role of AMP-activated protein kinase in mechanism of metformin action. J Clin Invest 108:1167–1174. https://doi.org/10.1172/JCI13505